Coherent Adiabatic Spin Control in the Presence of Charge Noise Using Tailored Pulses

Hugo Ribeiro, Guido Burkard, J. R. Petta, H. Lu, and A. C. Gossard

Coherent Adiabatic Spin Control in the Presence of Charge Noise Using Tailored Pulses

Hugo Ribeiro,[1] Guido Burkard,[1] J. R. Petta,[2, 3] H. Lu,[4] and A. C. Gossard[4]

[1]*Department of Physics, University of Konstanz, D-78457 Konstanz, Germany*
[2]*Department of Physics, Princeton University, Princeton, New Jersey 08544, USA*
[3]*Princeton Institute for the Science and Technology of Materials (PRISM),*
Princeton University, Princeton, New Jersey 08544, USA
[4]*Materials Department, University of California at Santa Barbara, Santa Barbara, California 93106, USA*

We study finite-time Landau-Zener transitions at a singlet-triplet level crossing in a GaAs double quantum dot, both experimentally and theoretically. Sweeps across the anti-crossing in the high driving speed limit result in oscillations with a small visibility. Here we demonstrate how to increase the oscillation visibility while keeping sweep times shorter than T_2^* using a tailored pulse with a detuning dependent level velocity. Our results show an improvement of a factor ~ 2.9 for the oscillation visibility. In particular, we were able to obtain a visibility of ~ 0.5 for Stückelberg oscillations, which demonstrates the creation of an equally weighted superposition of the qubit states.

The adiabatic theorem of quantum mechanics states that a quantum system will remain in its instantaneous eigenstate if the variation of a dynamical parameter is slow enough on a scale determined by the energy separation from other eigenstates [1]. However, there are systems for which adiabaticity breaks down resulting in a transition between states. The first result quantifying population change in such a process is due to independent works by Landau, Zener, Stückelberg, and Majorana [2–5]. They considered a coupled two-level quantum system whose energies are controlled by a time dependent external parameter, which is defined such that the system exhibits an anti-crossing of magnitude $\Delta = 2\lambda$ at $t = 0$. If the system is prepared in its ground state, $|0\rangle$, at $t = -\infty$ and swept through the anti-crossing by modifying the external parameter in such a way that the energy difference is a linear function of time, $\Delta E = \alpha t$, then the probability to remain in $|0\rangle$ at $t = \infty$ (in the diabatic basis) is given by $P_{\mathrm{LZSM}} = \mathrm{e}^{-\frac{2\pi\lambda^2}{\hbar\alpha}}$, which is known as the Landau-Zener(-Stückelberg-Majorana) (LZSM) non-adiabatic transition probability. Remarkably, this elegant solution, although valid only in the asymptotic limit for an infinitely long sweep, has demonstrated its accuracy in real physical systems for which the sweep has a finite duration [6].

Another success of the asymptotic formulation resides in an accurate description of LZSM interferometry. If the system is driven back and forth across an anti-crossing, it accumulates a Stückelberg phase that gives rise to periodic variations in the transition probability [6]. Although the exact accumulated phase can only be calculated by solving the time-dependent Schrödinger equation [7–10], a scattering approach assimilating the phase acquired in a single passage to a Stokes phase [11] nicely reproduces experimental results obtained in superconducting qubits [12], two-electron spin qubits at a singlet (S)-triplet (T$_+$) anti-crossing [13, 14], and in nitrogen-

vacancy centers in diamond [15].

Focusing on spin qubits, passage through a S-T$_+$ anti-crossing in the energy level diagram is analogous to a spin-dependent beam splitter [13]. There are two major challenges relating to quantum control of such systems. First, in two-electron double quantum dots (DQD), the S-T$_+$ anti-crossing is located near the $(1, 1) \leftrightarrow (2, 0)$ interdot charge transition, where $(N_{\mathrm{L}}, N_{\mathrm{R}})$ refer to the number of electrons in the left and right quantum dots. As a result, the singlet state involved in the spin-dependent anti-crossing is a superposition of $(1, 1)$ and $(2, 0)$ singlet states. Second, the magnitude of the splitting at the level anti-crossing is set by transverse hyperfine fields. To achieve LZSM oscillations with 100% visibility, the sweep through the anti-crossing would have to be performed on a timescale set by the electron spin decoherence time T_2^*. As a result, there is a tradeoff between adiabaticity and inhomogeneous dephasing. While there are several studies about dissipative adiabatic passages (see for instance [16–21]), it remains to be shown how to make a system less sensitive to dissipation while at the same time increasing adiabaticity.

In this Letter, we attempt to reconcile the contradiction between the need for a slow (adiabatic) passage susceptible to dissipation and a fast passage minimizing dissipation effects. Our approach is based on the observation that the biggest population change occurs in the vicinity of the anti-crossing. We have developed a multi-ramp pulse sequence that has a detuning dependent level velocity, which we refer to as "double hat" pulse [see Fig. 2(b)]. The slow level velocity portion of the pulse is chosen to coincide with the passage through the S-T$_+$ anti-crossing in order to increase the visibility of the quantum oscillations.

To demonstrate the advantages of "double hat" pulses, we consider a finite-time LZSM model [22]. In this model, there are three parameters that control the magnitude of P_{LZSM}. The dimensionless coupling $\eta = \lambda/\sqrt{\alpha\hbar}$ and the
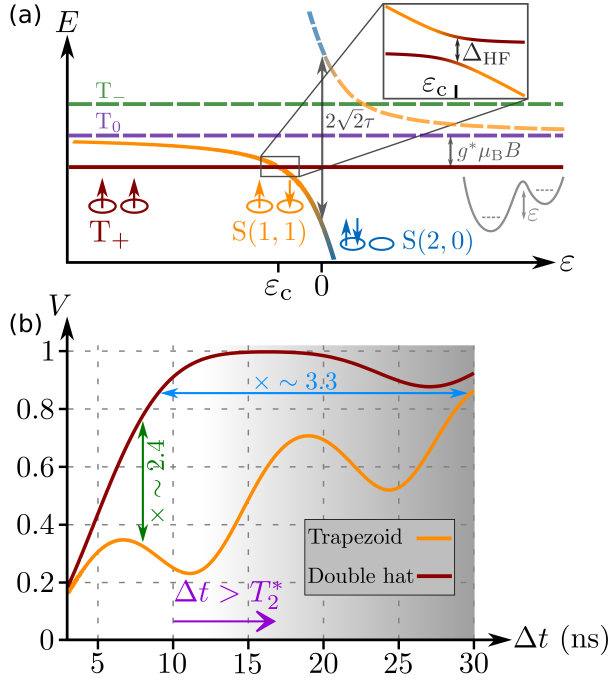
Figure 1. (color online) (a) DQD energy levels as a function of the detuning, ε, near the $(1,1) \leftrightarrow (2,0)$ charge transition. The low energy hybridized singlet state and the triplet T_+ form a qubit whose dynamics can be controlled through LZSM interferometry by sweeping the system through the hyperfine mediated anti-crossing. (b) Comparison of Stückelberg oscillation visibility V as a function of pulse length, Δt, for a trapezoid and "double hat" pulse with same maximal amplitude. The oscillation visibility is calculated within a finite-time LZSM model, where it is given by $V = 4P_{\text{LZSM}}(1 - P_{\text{LZSM}})$. "Double hat" pulses allow for more than a factor of two improvement while keeping $\Delta t < T_2^*$.

dimensionless initial and final times $T_{\text{i,f}} = \sqrt{\frac{\alpha}{\hbar}}t_{\text{i,f}}$, where $t_{\text{i,f}}$ are the start and stop times for the pulse relative to $t = 0$ defined at the anti-crossing. The dependence on $T_{\text{i,f}}$ results in oscillations of P_{LZSM}. In Fig. 1(b), we plot the visibility of Stückelberg oscillations, given by $V = 4P_{\text{LZSM}}(1 - P_{\text{LZSM}})$, as a function of pulse duration for trapezoid (single ramp) and "double hat" pulses. The duration of the pulse is increased by lowering the level-velocity α. For the "double hat" pulse, only the slow level velocity is changed. To be consistent with the regime studied in experiments, we choose $\lambda = 50\,\text{neV}$ and energy differences on the order of the Zeeman splitting ($-\Delta E_{\text{i}} = \Delta E_{\text{f}} = 2.5\,\mu\text{eV}$). The results demonstrate that "double hat" pulses can improve the oscillation visibility while maintaining a short pulse duration. The oscillation visibility is enhanced because "double hat" pulses allow a passage through the anti-crossing with a slower level velocity α as compare to trapezoid pulses. The oscillatory behavior of the results are a consequence of the finite-time LZSM model.

Ideally, one would like the visibility to be unity, which

corresponds to the perfect beam splitter limit, $P_{\text{LZSM}} = 0.5$. Its achievement would imply the possibility of realizing the Hadamard gate, which is essential to perform certain quantum algorithms (e.g. Shor's period finding algorithm [23]). Optimization methods to obtain high-fidelity adiabatic passages (i.e. $P_{\text{LZSM}} = 0$) have already been studied [24].

We measure and model LZSM transitions at the S-T_+ anti-crossing for finite duration sweeps. Measurements are performed on a GaAs/AlGaAs heterostructure that supports a two-dimensional electron gas located $110\,\text{nm}$ below the surface of the wafer. We use a triple quantum dot depletion gate pattern, where two of the dots are configured in series as a DQD and the third dot serves as a highly sensitive quantum point contact charge detector [13, 25]. The DQD is configured in the two-electron regime, where the electrons can either be separated in the $(1,1)$ configuration or localized on a single quantum dot, forming the $(2,0)$ charge state. In this regime, the spin states are the singlets S(2,0) and S(1,1) and the (1,1) triplet states T_+, T_0, and T_-. Interdot tunnel coupling τ results in hybridization of the charge states at zero detuning with a resulting splitting of magnitude $2\sqrt{2}\tau$ between a ground and excited state singlet, that we respectively denote S and S′. An external magnetic field is applied perpendicular to the sample, resulting in Zeeman splitting of the triplet states, as depicted in Fig. 1(a). The hyperfine interaction between electron and nuclear spins results in an anti-crossing between S and T_+ located at ε_{c}. The energy difference at the anti-crossing, Δ_{HF}, is set by transverse hyperfine fields [26].

Simulated interference patterns are obtained by solving the master equation $\dot{\rho} = -\frac{i}{\hbar}[H, \rho] + \frac{1}{2}\sum_{i=1}^{3}\left(\left[L_i\rho, L_i^\dagger\right] + \left[L_i, \rho L_i^\dagger\right]\right)$ [27]. Here, the Hamiltonian H describes the dynamics in the vicinity of the S-T_+ anti-crossing and is given by [28],

$$H(t) = E_{\text{S}}(t)|\text{S}\rangle\langle\text{S}| + E_{T_+}|T_+\rangle\langle T_+| + f(t)\left(|\text{S}\rangle\langle T_+| + \text{h.c}\right), \tag{1}$$

where E_{S} is the unperturbed singlet energy, $E_{T_+} = g^*\mu_{\text{B}}(B + B_{\text{HF},1}^z + B_{\text{HF},2}^z)$ is the triplet energy, with $g^* = -0.44$ the effective Landé g-factor, μ_{B} the Bohr magneton, B the external magnetic field, and $B_{\text{HF},j}^z$ the z-component of the hyperfine field in dot $j = 1, 2$. The effective coupling $f(t)$ between electronic spin states depends on the hyperfine interaction with nuclear spins and on the charge state. It can be written as $f(t) = c(t)\lambda$, with $c(t)$ the time-dependent $(1,1)$ charge amplitude and λ the hyperfine matrix element between S(1,1) and T_+. The Lindblad operators L_i are given by $L_1 = \sqrt{\Gamma_+}\sigma_+$, $L_2 = \sqrt{\Gamma_-}\sigma_-$, and $L_3 = \sqrt{\Gamma_\varphi}\sigma_z$. They respectively describe relaxation from excited to ground state and vice versa with rates $\Gamma_- = \gamma_1(n+1)$ and $\Gamma_+ = \gamma_1 n$ due to phonon emission and absorption, with the mean phonon number $n = (e^{\Delta E/k_{\text{B}}T} - 1)^{-1}$ and spontaneous spin relaxation rate $\gamma_1 = 1/T_1$, as well as pure dephasing with
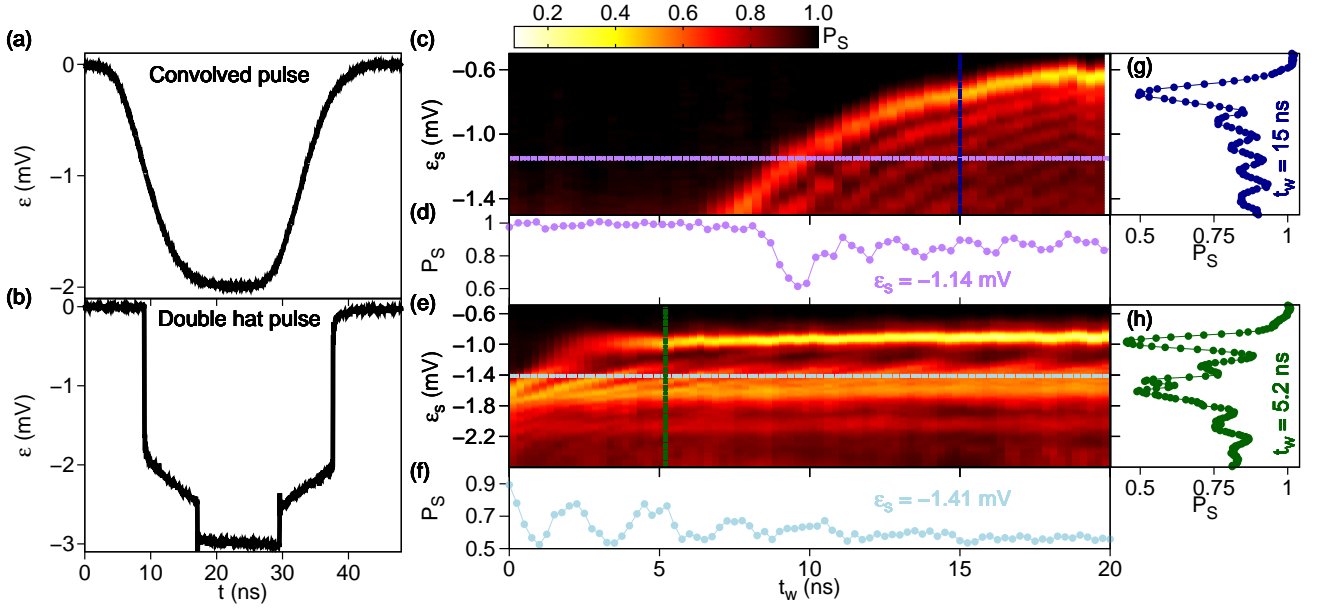
Figure 2. (color online) (a) Convolved pulse obtained by convolving a trapezoidal pulse with a Gaussian pulse. (b) "Double hat" pulse with a detuning-dependent level velocity. (c) Singlet return probability P_S as a function of ε_s and t_w for $B = 50\,\text{mT}$ using convolved pulses. (d) Trace taken along $\varepsilon_s = -1.14\,\text{mV}$. (e) Singlet return probability P_S measured with "double hat" pulses plotted as a function of ε_s and t_w for $B = 55\,\text{mT}$. The results exhibit a high-visibility region corresponding to slow level velocity portion of the "double hat" pulse. (f) Trace taken along $\varepsilon_s = -1.41\,\text{mV}$. This value of ε_s corresponds to a passage through the anti-crossing with the slow level velocity portion of the pulse. (g) and (h) Traces taken along $t_w = 15\,\text{ns}$ and $t_w = 5.2\,\text{ns}$ for convolved and "double hat" pulses respectively. A comparison between the different traces shows that the "double hat" pulse allows to achieve higher visibilities, while keeping the total pulse duration below the limit set by T_2^*.

a rate Γ_φ. A phenomenological model for the rates leads to the relation $\Gamma_+ + \Gamma_- = \gamma_1 \coth(\Delta E(t)/2k_B T)$, where $\Delta E(t)$ is the energy difference between the instantaneous eigenstates of Eq. (1), k_B is Boltzmann's constant, and T is the phonon bath temperature ($\sim 10\,\text{mK}$).

We furthermore assume that pure dephasing is mainly due to charge noise when the qubit is in a superposition of $S(2,0)$ and T_+. Since these two states have different orbital wave functions, they are sensitive to electric fluctuations of the charge background [29, 30]. We thus assume $\Gamma_\varphi = \gamma_2(1 - |c(t)|^2)$. The rates γ_1 and γ_2 are free parameters and can be used to fit experimental results. Nuclear spin induced dynamics are obtained by averaging solutions of the master equation over a Gaussian distribution of hyperfine fields [29, 31], suitable when the thermal energy is larger than nuclear Zeeman energy, $k_B T \gg g_n \mu_n B$, where g_n is the nuclear g-factor and μ_n is the nuclear magneton. This description of the nuclear state is only valid when its internal dynamics happens on characteristic time scales longer than those of the LZSM driven system (classical approximation). The standard deviation of the distribution of nuclear fields $B_{\text{HF},j}^i$ ($i = \{x, y, z\}$, $j = \{1, 2\}$) is denoted by δ_j^i. The singlet energy and charge amplitude coefficient used for our simulations are determined experimentally [13].

We consider two types of pulses to measure the singlet return probability P_S [13]. Convolved pulses which are

obtained by convolving a trapezoid pulse with a finite rise-time of 1.5 ns, a maximal amplitude of $-2\,\text{mV}$ and a variable width t_w, with a Gaussian pulse of mean $\mu = 0$ and standard deviation $s = 3.7\,\text{ns}$ [see Fig. 2(a)]. "Double hat" pulses are tailored to have a detuning-dependent level velocity at the leading and trailing edges of the pulse. The leading edge of the pulse has a level velocity that varies in the sequence fast-slow-fast. The leading edge has a rise-time of 0.1 ns and an amplitude of $-2\,\text{mV}$, which is followed by a slow ramp with a rise-time $t_{\text{slow}} = 8\,\text{ns}$ and amplitude of $-0.5\,\text{mV}$. A 0.1 ns rise-time pulse shifts the detuning to its maximal value of $-3\,\text{mV}$, where the detuning is held constant for a time interval t_w. The lever-arm conversion between gate voltage and energy is $\sim 0.13\,\text{meV/mV}$. The trailing edge of the pulse is simply the reverse of the leading edge [see Fig. 2(b)]. We present in Fig. 2(c) and (d) P_S as a function of final detuning ε_s and waiting time t_w obtained respectively with convolved pulses for $B = 50\,\text{mT}$ and "double hat" pulses for $B = 55\,\text{mT}$.

Since P_S for convolved pulses exhibits features already discussed in [13], we first only discuss the interference pattern obtained with "double hat" pulses. Since the maximal amplitude of these pulses does not depend on t_w, we can observe interference fringes that start at $t_w = 0\,\text{ns}$, which is a first step for manipulation within T_2^*. More importantly, we notice three distinct regions

4

for detunings smaller than $\varepsilon_c \sim -0.99\,\mathrm{mV}$, which correspond to different magnitude ranges for P_S. There is an alternation between regions with $P_S \simeq 1$, $P_S \simeq 0.4 \sim 0.9$, and again $P_S \simeq 1$ in correspondence with the different level velocities associated to the "double hat" pulse. A passage through the anti-crossing with a slower level velocity improves the oscillation visibility, as we could expect from the earlier considerations within finite-time LZSM theory.

To demonstrate that a high oscillation visibility can be achieved with "double hat" pulses, we compare two different types of traces. First, we compare traces taken for a fixed waiting time. This is equivalent to measuring the visibility of Stückelberg oscillations for a double passage as a function of ε_s. The results are presented in Figs. 2(g) and (h) for convolved pulses and "double hat" pulses. To compare quantitatively the visibility of the coherent oscillations, we have to neglect the final detuning $\varepsilon_s = \varepsilon_c$, which is strongly affected by relaxation mechanisms [28]. We thus find that the visibility for convolved pulses is ~ 0.17 and the visibility of "double hat" pulses is ~ 0.5, which corresponds to an improvement of a factor ~ 2.9. Second, we present a comparison of traces taken at a fixed value of detuning. This is equivalent to measuring the visibility of Rabi oscillations. The results are presented in Figs. 2(d) and (f) for convolved pulses and "double hat" pulses. Neglecting once more the first oscillation dip for convolved pulses that corresponds to the position of the avoided crossing [c.f. [13]], we find, by considering only the first peak and relevant dip, for convolved pulses a visibility of ~ 0.14 and for "double hat" pulses a visibility of ~ 0.4. Here, there is an improvement of a factor ~ 2.9, and which corresponds to the case $\Delta t \ll T_2^*$. By considering the first three peaks and dips, i.e. $\Delta t \sim T_2^*$, we find an improvement of ~ 2.4. The reduction of visibility is due to nuclear spin dephasing. We expect to obtain improvements in the visibility close to ~ 2.9 for suitably prepared nuclear states, which exhibit longer decoherence times. The error on the visibility is on the order of the error on P_S, which we find to be $\sim 7\%$.

To support our experimental findings, we present in Fig. 3 theory results obtained by using the experimental pulse profiles measured at the output port of the waveform generator. We use $\delta_{1,2}^{x,y,z} = 1.00\,\mathrm{mT}$, $\gamma_1 = 10^5\,\mathrm{s}^{-1}$, and $\gamma_2 = 10^8\,\mathrm{s}^{-1}$. Moreover, since the experimental data acquisition is done at high rate with cycles of 5 μs, we can observe a build up of nuclear polarization. To take this into account in our model, we allow a non-zero mean for $B_{\mathrm{HF},j}^i$. The mean $\xi_{1,2}^z \simeq 0.0\,\mathrm{mT}$ for $B_{\mathrm{HF},1,2}^z$ can be determined from spin-funnel measurements [13]. Since we cannot experimentally determine $\xi_{1,2}^{x,y}$, we have chosen $\xi_1^{x,y} = 6\,\mathrm{mT}$ and $\xi_2^{x,y} = 0\,\mathrm{mT}$. Our theory results agree qualitatively with the experiments, as can be seen when comparing interference fringes [see Figs. 3(a) and
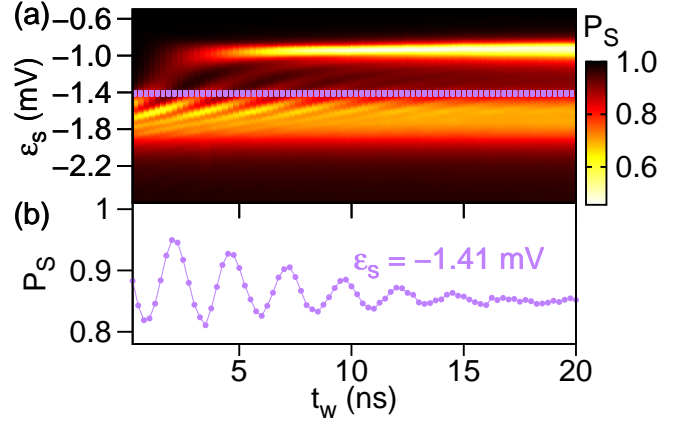

Figure 3. (color online) (a) Theoretical calculations of P_S as a function of t_w and ε_s for "double hat" pulses and $B = 55\,\mathrm{mT}$. Theory is in qualitative agreement with the experimental measurements. (b) Trace taken along $\varepsilon_s = -1.41\,\mathrm{mV}$.

2(e)].

Our results indicate that the qubit is not only influenced by nuclear spins, but that there are additional physical mechanisms that determine the oscillation visibility. Here, the contrast is also limited due to the superposition of S(2,0) and S(1,1) [28]. First, the weighting of S(1,1) sets the amount of population that can be transferred to T_+. Second, superpositions of different charge states are susceptible to charge noise, which results in an additional effective spin dephasing mechanism. This dephasing channel directly competes against LZSM tunneling by preventing the qubit from coherently interfering with itself. Spin relaxation also changes the balance of populations, but due to energy scales its effect is weak far from the avoided crossing, where $k_B T \ll \Delta E$.

In conclusion, we have demonstrated how to increase the visibility of quantum oscillations by enhancing the adiabatic passage probability in the presence of dissipation. We have designed a pulse which combines both fast and slow rise-time ramps to minimize dissipation and enhance adiabaticity. By considering a S-T_+ anti-crossing, we have shown that it is possible to achieve coherent superposition states with high T_+ population. In the more general context of LZSM driven spin qubits, this technique allows one to perform more quantum gates within a given decoherence time and achieve higher amplitude rotations in the qubit space without exponentially extending the gate operation times. Our control technique can be further improved by preparing a nuclear spin gradient [34]. This will not only increase T_2^*, but it will also enhance the effective coupling between spin states, thus boosting adiabatic transition probabilities.

———————————

[1] M. Born and V. A. Fock, Z. Phys. **51**, 165 (1928).
[2] L. D. Landau, Phys. Z. Sowjetunion **2**, 46 (1932).
[3] C. Zener, Proc. R. Soc. A **137**, 696 (1932).
[4] E. C. G. Stückelberg, Helv. Phys. Acta **5**, 369 (1932).
[5] E. Majorana, Nuovo Cimento **9**, 43 (1932).
[6] S. N. Shevchenko, S. Ashhab, and F. Nori, Physics Reports **492**, 1 (2010).
[7] H. Ribeiro and G. Burkard, Phys. Rev. Lett. **102**, 216802 (2009).
[8] J. Särkkä and A. Harju, N. J. Phys. **13**, 043010 (2011).
[9] G. D. Fuchs, G. Burkard, P. V. Klimov, and D. D. Awschalom, Nat. Phys. **7**, 789 (2011).
[10] S. A. Studenikin, G. C. Aers, G. Granger, L. Gaudreau, A. Kam, P. Zawadzki, Z. R. Wasilewski, and A. S. Sachrajda, Phys. Rev. Lett. **108**, 226802 (2012).
[11] R. E. Meyer, SIAM Review **31**, 435 (1989).
[12] W. D. Oliver, Y. Yu, J. C. Lee, K. K. Berggren, L. S. Levitov, and T. P. Orlando, Science **310**, 1653 (2005).
[13] J. R. Petta, H. Lu, and A. C. Gossard, Science **327**, 669 (2010).
[14] L. Gaudreau, G. Granger, A. Kam, G. C. Aers, S. A. Studenikin, P. Zawadzki, M. Pioro-Ladrière, Z. R. Wasilewski and A. S. Sachrajda, Nat. Phys. **8**, 54 (2012).
[15] P. Huang, J. Zhou, F. Fang, X. Kong, X. Xu, C. Ju, and J. Du, Phys. Rev. X **1**, 011003 (2011).
[16] P. Ao and J. Rammer, Phys. Rev. Lett. **62**, 3004 (1989).
[17] E. Shimshoni and Y. Gefen, Ann. Phys. **210**, 16 (1991).
[18] M. Wubs, K. Saito, S. Kohler, P. Hänggi, and Y. Kayanuma, Phys. Rev. Lett **97**, 200404 (2006).
[19] K. Saito, M. Wubs, S. Kohler, Y. Kayanuma, and P. Hänggi, Phys. Rev. B **75**, 214308 (2007).
[20] P. Nalbach and M. Thorwart, Phys. Rev. Lett. **103**, 220401 (2009).
[21] P. P. Orth, A. Imambekov, K. Le Hur, Phys. Rev. A **82**, 032118 (2010).
[22] N. V. Vitanov and B. M. Garraway, Phys. Rev. A **53**, 4288 (1996).
[23] P. Shor, SIAM Journal of Computing **26**, 1484 (1997).
[24] B. T. Torosov, S. Guérin, and N. V. Vitanov, Phys. Rev. Lett. **106**, 233001 (2011).
[25] See supplemental material for more details.
[26] J. M. Taylor, J. R. Petta, A. C. Johnson, A. Yacoby, C. M. Marcus, M. D. Lukin, Phys. Rev. B **76**, 035315 (2007).
[27] G. Lindblad, Commun. Math. Phys. **48**, 119 (1976).
[28] H. Ribeiro, J. R. Petta, and G. Burkard, arXiv:1210.1957 (2012).
[29] W. A. Coish and D. Loss, Phys. Rev. B **72**, 125337 (2005).
[30] X. Hu and S. Das Sarma, Phys. Rev. Lett. **96**, 100501 (2006).
[31] A. V. Khaetskii, D. Loss, and L. Glazman, Phys. Rev. Lett. **88**, 186802 (2002).
[32] J. R. Petta, A. C. Johnson, J. M. Taylor, E. A. Laird, A. Yacoby, M. D. Lukin, C. M. Marcus, M. P. Hanson and A. C. Gossard, Science **309**, 2180 (2005).
[33] H. Ribeiro, J. R. Petta, and G. Burkard, Phys. Rev. B **82**, 115445 (2010).
[34] S. Foletti, H. Bluhm, D. Mahalu, V. Umansky, A. Yacoby, Nat. Phys. **5**, 903 (2009).